Video Article

Ferric Chloride-induced Murine Thrombosis Models

Wei Li[1,2], Marvin Nieman[3], Anirban Sen Gupta[4]

[1]Department of Cellular and Molecular Medicine, Lerner Research Institute, Cleveland Clinic

[2]Department of Molecular Medicine, Cleveland Clinic Lerner College of Medicine of Case Western Reserve University

[3]Department of Pharmacology, Case Western Reserve University

[4]Department of Biomedical Engineering, Case Western Reserve University

Correspondence to: Wei Li at liw4@ccf.org

Abstract

Arterial thrombosis (blood clot) is a common complication of many systemic diseases associated with chronic inflammation, including atherosclerosis, diabetes, obesity, cancer and chronic autoimmune rheumatologic disorders. Thrombi are the cause of most heart attacks, strokes and extremity loss, making thrombosis an extremely important public health problem. Since these thrombi stem from inappropriate platelet activation and subsequent coagulation, targeting these systems therapeutically has important clinical significance for developing safer treatments. Due to the complexities of the hemostatic system, *in vitro* experiments cannot replicate the blood-to-vessel wall interactions; therefore, *in vivo* studies are critical to understand pathological mechanisms of thrombus formation. To this end, various thrombosis models have been developed in mice. Among them, ferric chloride ($FeCl_3$) induced vascular injury is a widely used model of occlusive thrombosis that reports platelet activation and aggregation in the context of an aseptic closed vascular system. This model is based on redox-induced endothelial cell injury, which is simple and sensitive to both anticoagulant and anti-platelets drugs. The time required for the development of a thrombus that occludes blood flow gives a quantitative measure of vascular injury, platelet activation and aggregation that is relevant to thrombotic diseases. We have significantly refined this $FeCl_3$-induced vascular thrombosis model, which makes the data highly reproducible with minimal variation. Here we describe the model and present representative data from several experimental set-ups that demonstrate the utility of this model in thrombosis research.

Video Link

The video component of this article can be found at http://www.jove.com/video/54479/

Introduction

Arterial thrombosis (blood clot) is a common complication of many systemic diseases associated with chronic inflammation, including atherosclerosis, diabetes, obesity, cancer and chronic autoimmune rheumatologic disorders. Thrombi that occur in the arterial circulation stem from inappropriate platelet activation, aggregation and subsequent coagulatory mechanisms, and are implicated in heart attacks, strokes and extremity loss. The vessel wall is a complex system that includes multiple cell types and is influenced by a multitude of extrinsic factors including shear stress, circulating blood cells, hormones and cytokines, as well as expression of antioxidant proteins in the vessel wall. *In vitro* experiments cannot replicate this complex environment and therefore *in vivo* studies using animal models are critical to allow better understanding of mechanisms involved in thrombotic disorders.

Mice have been shown to have similar mechanisms to humans in terms of thrombosis, atherosclerosis, inflammation and diabetes[1,2]. Furthermore, transgenic and knockout mice can be created to test the function of specific gene products in a complex physiologic or pathologic environment. Such studies mimic human pathology and may provide important mechanistic information related to discovery of new pathways and therapies, as well as provide important details in characterizing drug effects on thrombosis.

Pathological arterial thrombi occur due to endothelial layer injury or dysfunction and exposure of the blood stream to the subendothelial matrix[3,4]. Various thrombosis models have been developed to induce this endothelial damage such as mechanical injury, photoreactive compound Rose Bengal-based oxidative injury and laser injury[5]. In this spectrum, Ferric chloride ($FeCl_3$)-induced vascular injury is a widely used model of thrombosis. This reagent when applied to the outer aspect of vessels induces oxidative damage to vascular cells[6-8], with loss of endothelial cell protection from circulating platelets and components of the coagulation cascade. The $FeCl_3$ model is simple and sensitive to both anticoagulant and anti-platelets drugs, and has been performed on carotid and femoral arteries, jugular veins, and mesenteric and cremasteric arterioles and venules in mice, rats, guinea pigs and rabbits[6-15].

One measurable parameter in this model is the elapsed time from injury to complete vessel occlusion, measured as blood flow cessation with a Doppler flow meter or under direct observation with intravital microscopy[6,7,9]. A range of times between 5 to 30 min has been reported in different

studies in C57Bl6 mice[7-10,16], suggesting that $FeCl_3$ concentrations, types of anesthesia, surgical techniques, mouse age, genomic background, method of measuring blood flow, and other environmental variables have significant effects in this model. This wide variability makes it difficult to compare studies from different research groups and may make detection of subtle differences difficult.

With a vision to minimize such variabilities and establish a uniformly reproducible *in vivo* model system, we have refined the $FeCl_3$-induced carotid artery model that makes the data highly reproducible with minimal variation[6-10,16-19]. In this paper we describe and share the skills and report several representative experimental examples that can benefit from this model.

Protocol

All procedures and manipulations of animals have been approved by Institutional Animal Care and Use Committees (IACUC) of The Cleveland Clinic in accordance with the United States Public Health Service *Policy on the Humane Care and Use of Animals*, and the NIH *Guide for the Care and Use of Laboratory Animals*.

1. Preparations:

1. **Fluorescent Dye for Labeling Platelets**
   1. Prepare rhodamine 6G solution, 0.5 mg/ml, in saline and sterilize the solution with 0.22 μm filter.

2. **$FeCl_3$ Solution**
   1. Make a fresh stock solution of 30% $FeCl_3$ (Anhydrous, equals 1.85 M) in pure water, and filter with 0.45 μm filter. Prepare 5 ml fresh $FeCl_3$ solution at the desired concentration [*e.g.,* 2.5% (0.154 M), 5% (0.308 M), 7.5% (0.463 M), 10% (0.617 M) and 12.5% (0.771 M)] by diluting the 30% $FeCl_3$ solution with water in a 6 cm tissue culture dish and keep the lid closed.
   NOTE: Using the culture dish makes it easier to pick up the filter paper saturated with $FeCl_3$ solution than to pick it up from a narrow container, such as a 1.5 ml microcentrifuge tube. FeCl3 is extremely hazardous and that precautions, such as wearing gloves and lab coat etc., Personal Protective Equipment, should always be taken.

3. **Filter Papers**
   1. Cut the filter paper to 1 mm x 2 mm size. Soak enough pieces of the cut filter paper in the $FeCl_3$ solution in the same dish.

4. **Papaverine Hydrochloride Solution**
   1. Prepare papaverine hydrochloride solution (25 mg/ml) in water and sterilize the solution with 0.22 μm filter.

5. **Agarose Gel**
   1. Prepare 2% agarose gel in PBS or saline in 6-well tissue culture plate, ~ 1 cm thickness, and cut it to half-circle with ~ 3 cm diameter.

2. $FeCl_3$ Induced Carotid Arterial Injury Thrombosis Model

1. **Surgical Procedures for the Thrombosis Model**
   1. Use 8 - 12 weeks old C57Bl6 mice (or other strains as necessary). Anesthetize mice with the mixture of ketamine (100 mg/kg)/xylazine (10 mg/kg) via intraperitoneal injection. Confirm the depth of the anesthesia by toe pinching.
   NOTE: This amount of ketamine/xylazine is sufficient to keep the animal in stable anesthesia and no pain (response to toe pinching) for at least 1 hr.
   2. Remove fur on the neck and upper chest with a small animal electric clipper. Depilatory cream is not necessary. Apply neutral petroleum eye ointment on the eyes to prevent dryness during anesthesia.
   3. Secure the mouse in the supine position on the lid of 15 cm tissue culture plate. Use one long tape (~ 10 cm) to secure hind limbs and lower body, and two pieces of small tape (2 cm x 0.5 cm) to secure forelegs. Use a 4-0 suture to wrap around the incisors, tape the two ends of the suture to the lid to keep mouse neck straight (**Figure 2**).
   4. Place plate with mouse head toward the operator under a surgical light source.
   5. Sterilize the surgical site with alcohol pad. Use the Micro-Adson Forceps to hold the skin and use a surgical scissors to make a small incision (2 - 3 mm).
   6. Hold the skin of the incision with the forceps and insert surgical scissors with jaws closed into the incision. Push the scissors subcutaneously toward the manubrium or chin, and then open the scissors to free the skin from the subcutaneous layer.
   7. Cut the skin with the surgical scissors to make a midline incision from the manubrium to the level of hyoid bone (**Figure 3A** and **3B**). Bluntly dissect the thin fascia (dotted line, in **Figure 3B**) between the submaxillary glands with a fine hemostat and a Graefe forceps (**Figure 3B** and **3C**; **blue arrows**).
   NOTE: The manubrium (black arrow in **Figure 3C**) and the trachea (T in **Figure 3C**) will be seen after this step.
   8. Hold the soft tissue and the skin seen at the right of the manubrium with the Graefe forceps, insert the hemostat under the fascia toward the 2 o'clock position (**yellow dotted line in Figure 3C**), open the jaws of the hemostat to free the jugular vein from surrounding tissue.
   9. Cut the fascia, soft tissue and skin toward the 2 o'clock position (**Figure 3C**) with the surgical scissors to expose the right jugular vein (**Figure 3D, arrow**).
   10. Draw about 200 - 300 μl rhodamine 6G solution using a 1 ml syringe with 22 G needle, and then change it to 30 G needle.
   NOTE: This protects the 30 G needle from damage of its fine tip. Directly drawing the rhodamine 6G solution with the 30 G needle will not damage the tip; however touching the container wall accidentally will cause damage, which may make injection difficult.
   11. Flush the 30 G needle by slowly pushing out the rhodamine 6G solution, make sure no air bubbles remain in the syringe or the needle. Keep 100 μl rhodamine 6G solution for injection.

12. Bend 2 - 3 mm tip of the needle to a 90° angle with the needle holder, which will prevent inserting the needle too deep to the jugular vein and makes the injection more easily controlled (**Figure 3D**).
13. Inject the rhodamine 6G solution into the right jugular vein to label platelets. To stabilize the syringe and keep the needle in position, hold the syringe with one hand and the needle with the Graefe forceps with another hand during the injection.After injection, clamp the injection site with the Graefe forceps to avoid bleeding.
14. Open the jaws of the hemostat and insert it under the Graefe forceps to clamp the vessel wall of the injection site, and then ligate the injection site with a 6-0 suture.
    NOTE: As an alternative of step 2.1.15, applying pressure to the injection site with a finger for 2 min will stop the bleeding; however, this method has a risk of causing further bleeding if the clot at the injection site is removed accidently.
15. Bluntly dissect the soft tissue and fascia around the left submaxillary gland with the hemostat and the Graefe forceps and pull the gland toward the 7 o'clock position (**Figure 3E**) to expose the left sternocleidomastoid muscle (blue arrow in **Figure 3E**).
16. Bluntly dissect the fascia (**Figure 3E, dotted line**) between the left sternocleidomastoid muscle and the omohyoid muscle or the sternohyoid muscle (**Figure 3E, green arrow**) located to the left site of the trachea with the hemostat.
17. Pass a needle with 6-0 silk suture (about 15 cm long) under the middle of the sternocleidomastoid muscle (blue arrow in **Figure 3E**), put the two ends of the suture together and pull the suture laterally toward the 10 o'clock position.
    NOTE: This procedure should be performed carefully to avoid injury of the left jugular vein, which is located outside of the sternocleidomastoid muscle.
18. Bluntly separate the thin sternohyoid muscle and/or omohyoid muscle to expose the carotid artery (CA) (**Figure 3F** arrow) after pulling away the sternocleidomastoid muscle. Cut the sternohyoid muscle and/or omohyoid muscle as necessary. Use the hemostat to separate the soft tissue from CA without touching the CA.
    NOTE: CA is accompanied by the vagus nerve, the white structure seen in **Figure 3G** (green arrow), and in most cases it is under the thin sternohyoid muscle and/or omohyoid muscle (between the yellow dotted lines in **Figure 3F**).
19. Use a fine tip forceps to pick up the lateral fascia around the CA while avoiding the vagus nerve and CA. Use another fine tip forceps to punch a hole on the fascia between the CA and vagus nerve.
20. Pass the hook through the hole and gently lift the CA, and then place the fine tip forceps under the CA. Move the hook and forceps in opposite directions along the CA to strip adventitial soft tissue. Free at least ~ 5 mm length of CA (**Figure 3H, blue arrow**) from surrounding tissue.
21. To block background fluorescence, press the end of a black plastic coffee stirrer to flat, crosscut the coffee stirrer into a 3 mm piece, and then cut longitudinally along the fold edges to get two pieces of "U" shape plastic (**Figure 3H, green arrow**).
22. Rinse one piece of this "U" shape plastic with saline and hold it with forceps and place it under the CA while gently lifting the CA with the hook (**Figure 3H, green arrow**). Immediately apply 2-3 drops of saline to avoid drying the CA.

2. **Real time Recording Video**
   1. Transfer the mouse and plate lid together to the microscope stage and place in an appropriate position under the 10X water lens. Fill the space between the 10X lens and the CA with saline.
   2. Start the digital video recording software application, and launch a new file and name it accordingly. Record normal vessel images and write down the frame number when the video recording is stopped.
      NOTE: Reference the video recording software in the computer for recording. We use digital video recording software and the following descriptions are based on this application.
      NOTE: Since mechanical trauma can injure the endothelium and lead to thrombus formation[20], it is necessary to confirm that there is no surgical injury to the vessel wall prior to the $FeCl_3$ injury. It is also necessary to confirm that there is no remaining tissue around the CA, which may form a barrier and attenuate the effect of $FeCl_3$-induced injury. Write down the frame number of the records will make it easy to analyze the videos according elapsed times later.
   3. Move the mouse with plate lid out of the 10X lens. Fold a corner of a paper towel to make a thin and fine tip and use it to carefully blot the saline around the CA (avoid touching CA) as well as in other places in the surgical field. This is important to avoid dilution of the $FeCl_3$ solution used.
   4. Use a fine tip forceps and pick up a piece of filter paper saturated with $FeCl_3$ solution and place it directly on the CA and keep it on site for 1 min.
      NOTE: To aid visualization of the bloodstream and harvest accurate data, place the filter paper close to the distal end of the exposed CA (**Figure 3I**) and leave a short segment at the proximal site (**green arrow in Figure 3I**) for observing blood flow at late phase (see below).
   5. Remove the filter paper (this time point is defined as the start of "after injury") and rinse the CA with saline (at least 2 ml).
   6. Put the mouse with plate lid back to the 10X lens; observe the vessel and start to record video images. Write down the video frame number at the end of the first minute of recording.
      NOTE: Thrombus formation is identified by accumulation of the fluorescent platelets, which is observed in real-time video images on computer screen or under microscope. Record video images immediately after putting the mouse back under the microscope. Keep recording to the end of the first minute after removing the filter paper. Observe the entire vessel from the distal to the proximal sites to obtain information about the injury, and then focus on the area of interest (usually is the center of the injured area) for further imaging.
   7. Record video images for 10 sec every minute for the first 10 min (*e.g.,* 2:55 to 3:05) and then 10 sec every other minute until the end of the experiment. Write down the frame numbers when each recording is stopped.
      NOTE: The end points of the model are: 1) when blood flow has ceased for > 30 sec; or 2) if occlusion is not seen in 30 min after injury. In this case, use 30 min for statistical analysis. Set Exposure Time of the video record as 10 msec at the beginning, so it will be easy to observe the blood flow over the thrombi. When the thrombi become large and the fluorescence saturates the camera's sensor, it becomes difficult to identify the blood flow over thrombi. To solve this issue, move the imaging center to the proximal uninjured site (**Figure 3I**, green arrow) where blood flow can still be clearly observed. We also increase the Expose Time to 15 or 20 msec when focusing on the proximal un-injured site, so the blood flow can be observed more clearly. When blood flow will cease, numerous larger cells (leukocytes) start to roll on the vessel wall at the proximal site of the thrombus. Flow usually stops within 2 - 3 min after the appearance of the large cells. Write down the Expose Time on the recording sheet if it is changed. It usually takes about 30 min from the anesthesia to the end of the experiment, if the normal wild type C57Bl6 mice were used.

CAUTION NOTE: Don't use the white aggregated platelet clot as the sign of the blood flow cessation, which will not give an accurate data and it is affected by the exposure time. The white clot covered the vessel lumen does not mean blood flow ceased (see the representative video 1).

8. At the end of experiment, euthanize the mice using overdose ketamine/xylazine (200/20 mg/Kg), followed by cervical dislocation after confirming no breath and heartbeat.

3. FeCl$_3$ Induced Mesenteric Artery/Vein Thrombosis Model

1. Anesthetize 8 − 12 week old C57Bl6 mice as mentioned in section 2.1.1. Apply vet ointment on the eyes to prevent dryness during anesthesia.
2. Inject Papaverine solution (total 0.4 mg/mouse) intraperitoneally to inhibit gut peristalsis.
3. Remove fur on the neck and abdomen with an animal electric clipper. Depilatory cream is not necessary.
4. Secure the mouse in the supine position on the lid of 15 cm tissue culture plate. Use four pieces of small tape (2 cm x 0.5 cm) to secure all legs. Use a 4 -0 suture to wrap around the incisors, tape the two ends of the suture to the lid to keep the neck straight (**Figure 2**).
5. Follow procedures 2.1.4 - 2.1.15 to expose the jugular vein for injection of rhodamine 6G to label platelets.
6. Perform a midline incision through the skin from xiphoid to lower abdomen using the surgical scissors (**Figure 4A**). Pick up the middle peritoneum (also called linea alba, **Figure 4A**, arrow) with Graefe forceps, which is clear and has no blood vessels, lift about 2 - 3 mm high, confirm no bowel under the cutting line, and cut the peritoneum open longitudinally with the fine scissors (**Figure 4B**).
7. Re-secure the mice to right lateral position. Place the half-circle agarose gel close to the abdomen, and gently exteriorize the intestines and spread it on the top of the gel with the Graefe forceps (**Figure 4C**). Use the second branches for the thrombosis experiment (**Figure 4C, arrow**).
   NOTE: Use the hemostat or Micro-Adson forceps to help to exteriorize the intestines. Avoid hurting the bowel and the vessel.
8. Place 5 - 6 drops saline to keep the moisture of the bowel and vessel. Transfer the mouse with the plate lid together to the microscope stage and place in appropriate position under the 10X dry lens.
   NOTE: Use a dry lens because the jejunoileal membrane cannot hold saline solution. Make sure to drop saline solution on the exposed tissues to keep them moist.
9. Blot the saline around the mesenteric artery and vein before treatment.
10. Use a fine tip forceps to pick up a piece of filter paper saturated with 12.5% FeCl$_3$ solution and place it directly on the mesenteric artery and vein for 1 min (**Figure 4D**). Remove the filter paper (this time point is defined as the start of "after injury") and rinse the injured mesenteric artery and vein with saline (at least 2 ml).
11. Put the mouse with plate lid back under the 10X dry lens; observe the vessels and start to record video images as mentioned in 2.2).
    NOTE: The end points of this experiment are: 1) when blood flow has ceased for > 30 sec; or 2) if occlusion is not seen in 30 min after injury, and in this case use 30 min for statistical analysis.
12. At the end of experiment, euthanize the mice using overdose ketamine/xylazine (200/20 mg/Kg), followed by cervical dislocation after no breath and heart beating are confirmed.

Representative Results

Carotid Artery Thrombosis Model
In mice with C57BL6 background, we recommend using 7.5% FeCl$_3$ to treat the vessel for 1 min as a starting point. Under treatment of 7.5% FeCl$_3$, borders of the injured area and normal vessel wall are easily identified under microscope (See **online video 1**), suggesting that the endothelial layer was significantly damaged. The thrombi formed immediately upon FeCl$_3$ treatment, and are observed in all WT C57BL6 mice 1 min after injury. The initially formed thrombi are unstable and parts of them are usually washed away by the blood stream, so the formed thrombi become smaller at 2 - 3 min after injury. Thrombi start to enlarge from 3 - 4 min after removing the filter paper and these later formed thrombi are stable and usually are not washed away. The average occlusive time is 11.3 ± 3.16 min in the C57BL6 mice (n= 14) when 7.5% FeCl$_3$ is used[6,7,19] (**Figure 5A** and **online video 1**). In the previous studies we have demonstrated that both decrease and increase of FeCl$_3$ concentrations diminish the difference between an anti-thrombotic mouse strain and WT mice[6]; From our experience, treatment of the carotid artery with 7.5% FeCl$_3$ for 1 min is sufficient to satisfy all of our purposes. In addition to test function of specific genes using knockout mice[7,8,16,19,21], following are four representative experiments using this model:

Intravenous Perfusion of tissue-type Plasminogen Activator Mediated Thrombolysis
Tissue-type plasminogen activator (tPA) is one of the FDA-approved drugs for thrombolysis treatment in the United States[22]. We thus observed the tPA-mediated thrombolysis in the carotid artery thrombosis model. Thrombosis was initiated with 7.5% FeCl$_3$ and allowed to form for 5 min before tPA (1 mg/Kg body weight) was perfused via a jugular vein catheter (22GA). As shown in **Figure 5B** and **online video 2**, the thrombus continually magnified and occupied about 50% of the lumen 5 min after injury. The thrombi continued to enlarge after tPA perfusion suggesting that tPA does not affect platelet activation and aggregation. Thrombolysis started about 4 minutes after tPA injection. The formed thrombi were found to undergo size variations repeatedly during the 30 min observation period and no vessel occlusion happened in this case. These data clearly showed that tPA cannot completely inhibit platelet-mediated thrombus formation, even if it leads to thrombolysis. Therefore, we envision that future experiments utilizing the FeCl$_3$-induced arterial thrombosis model can be utilized to evaluate thrombolytic and other adjunctive therapies that can have a prominent preventative effect on thrombus formation.

Perfusion of PAR4 Antibody to Mice Inhibits Thrombosis

Protease activated receptor 4 (PAR4) is a G protein coupled receptor (GPCR) on platelets which is activated by proteolytic cleavage of its N-terminal exodomain[23] and subsequently leads to steps in platelet activation. The Nieman lab has generated a goat polyclonal PAR4 antibody (CAN12) that targets the anionic cluster of PAR4, and delays PAR4 cleavage, thereby affecting a critical step for PAR4 mediated platelet activation[24]. By perfusion of 1 mg/Kg of this antibody to the C57BL6 mice, we found that inhibition of PAR4 cleavage significantly prolonged times to occlusive thrombus formation in the 7.5% $FeCl_3$ induced carotid artery thrombosis model (**Figure 5C** and **online video 3**). This demonstrates that the $FeCl_3$-induced thrombosis model can be utilized to evaluate the effects of anti-platelet agents and characterize potential therapeutic strategies.

Nanoparticle-mediated Thrombi-specific Targeting

Rapid clot-removal to re-establish blood flow is crucial in treating occlusive vascular diseases including ischemic stroke and myocardial infarction. Systemic delivery of thrombolytic drugs, such as tPA showed above, can lyse the formed thrombi, but cannot completely prevent platelet activation and re-aggregation/occlusion. Additionally, systemic direct delivery of such serine protease agents can lead to indiscriminate off-target action, leading to major side effects including hemorrhage. The Sen Gupta lab has engineered platelet-inspired nanoparticle-based synthetic delivery vehicles that can bind to clot-associated activated platelets and proteins under hemodynamic shear flow[25-27]. We thus examined whether these nanoparticles can bind to the actively forming thrombi in an artery.

As mentioned in experiment for tPA perfusion, a catheter was inserted into the jugular vein and connected to an Injection Pump for injection of nanoparticle at uniform flow rate. In this experiment, no fluorescence dye was injected into the mouse to label platelets. Instead, the nanoparticles were labeled with Rohdamine B; therefore they were able to be observed under intravital microscope. The thrombosis was initiated with 7.5% $FeCl_3$ treatment for 1 min as mentioned previously. Since in WT mice, a significant amount of thrombi was found to form 5 min after injury, we selected this time point for injection of nanoparticles to detect if the nanoparticles bind efficiently to the actively forming thrombi. As shown in **Figure 5D** and **online video 4**, after injection of fluorescent nanoparticles, we were able to identify a mountain-shaped thrombus which got progressively covered by the fluorescent particles. These studies demonstrate the utility of the $FeCl_3$-induced thrombosis model to evaluate the targeting capability (and subsequent therapeutic efficacy) of clot-targeted particulate drug delivery systems.

### Role of Red Blood Cells other than Platelets in Thrombus Formation.

Recent studies have suggested that red blood cells (RBCs) play important role in the $FeCl_3$ induced thrombosis model[28] and they are the first adherent blood component to the injured vessel wall[29,30]. To explore this phenomenon, we labeled RBCs with 1,1'-Dioctadecyl-3,3,3',3'-Tetramethylindocarbocyanine Perchlorate (Dil, 10 µM final concentration). The Dil-labeled RBCs were washed two times with PBS and resuspended in saline with 35% hematocrit. The Dil-labeled RBC suspension (100 µl per mouse) was injected into the thrombocytopenic mice which have been lethally irradiated 5 days before the experiment[19]. These thrombocytopenic mice have significant decreased platelets, which will increase the chance of RBC biding to the vessel wall, if they do. In contrast to the experiments using fluorescence-labeled platelets (**Figure 5**), no obvious accumulation of fluorescent cells was found on the vessel wall after vascular injury (**Figure 6A**, **online video 5**). However, along with the formation of the platelet-rich thrombi, RBCs started to accumulate in the thrombus which illustrates the shape of the clot (**Figure 6A**). Immunofluorescence staining of the injured carotid artery demonstrated that the major cells adhered to the vessel wall are platelets (CD41 positive, green), while the Dil-labeled RBCs are mainly trapped within the thrombi (**Figure 6B & C**). These studies demonstrate that the $FeCl_3$-induced thrombosis model can be utilized in gaining mechanistic insight on cellular and molecular components and spatio-temporal events in thrombus formation.

Mesenteric Thrombosis Model

For the mesenteric thrombosis model, a high concentration of $FeCl_3$ (10 - 12.5%) is recommended as the vessels are usually surrounded by fat tissue, which can hinder the $FeCl_3$ diffusion towards the vessel wall and thus prevents vessel from $FeCl_3$-induced injury[7]. This model is more suitable for venous thrombosis study. As shown in **online video 6**, thrombus was seen around ~15 sec in the mesenteric vein after topically applying the filter paper saturated with 12.5% $FeCl_3$ solution, but thrombus formation is dramatically delayed in the mesenteric artery. The average time to occlusive thrombus formation is ~17 ± 7.2 min (n = 11) in mesenteric vein and about 23 ± 9.9 min (n = 10) in mesenteric artery when 12.5% $FeCl_3$ is used[7].


Figure 1. Surgery Tools. The minimal necessary tools for mouse surgery are shown. See Materials list for more detailed information. Please click here to view a larger version of this figure.
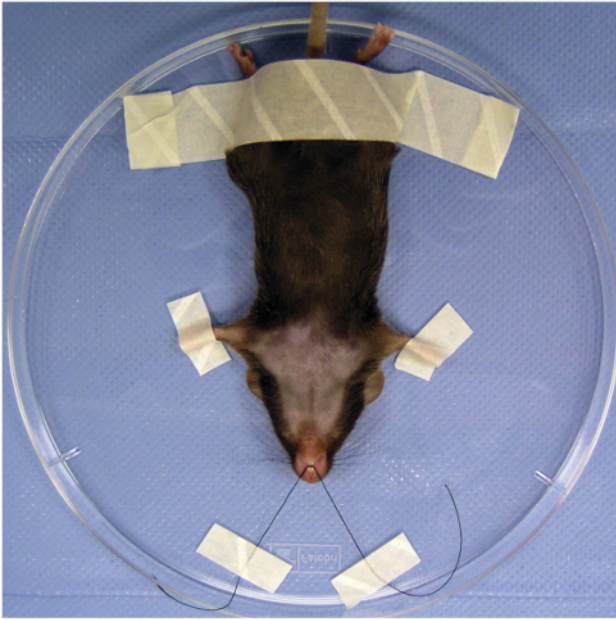
Figure 2. Mouse Fixation for Surgery. Secure the mouse on the 15 cm culture dish lid for carotid artery thrombosis model or for the injection of rhodamine 6G dye for the mesenteric thrombosis model. Please click here to view a larger version of this figure.
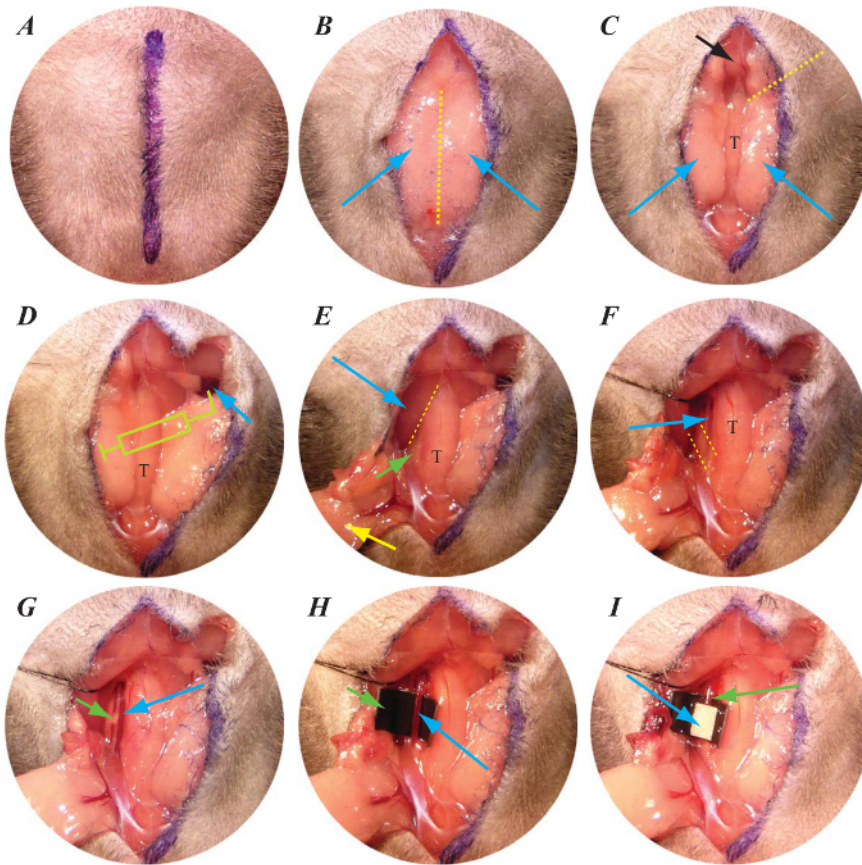
Figure 3. Carotid Artery Thrombosis Model. Procedures to expose the jugular vein, injection of rhodamine 6G florescent dye into the blood system and exposure of left carotid artery are shown. In **(A)**, the line indicates the incision from manubrium to the level of the hyoid bone; in **(B)**, blue arrows indicate submaxillary glands, and yellow dotted lines represent the fascia between the submaxillary glands; in **(C)**, blue arrows indicate submaxillary glands, black arrow indicates manubrium, and dotted yellow line indicates the position to cut to expose the jugular vein; in **(D)**, blue arrow indicates jugular vein; in **(E)**, yellow arrow indicates left submaxillary gland, blue arrow indicates left sternocleidomastoid muscle, dotted yellow line indicates fascia, and green arrow indicates the omohyoid muscle or the sternohyoid muscle; in **(F)**, blue arrow indicates carotid artery, the yellow dotted lines show the thin sternohyoid muscle and/or the omohyoid muscle; in **(G)**, the blue arrow indicates carotid artery and green arrow indicates vagus nerve; in **(H)**, the blue arrow indicates carotid artery and the green arrow indicates the plastic "U-shape" coffee stirrer; and in **(I)**, the blue arrow indicates the filter paper situated with FeCl₃ solution, and green arrow indicates the carotid artery. T indicates trachea. Please click here to view a larger version of this figure.
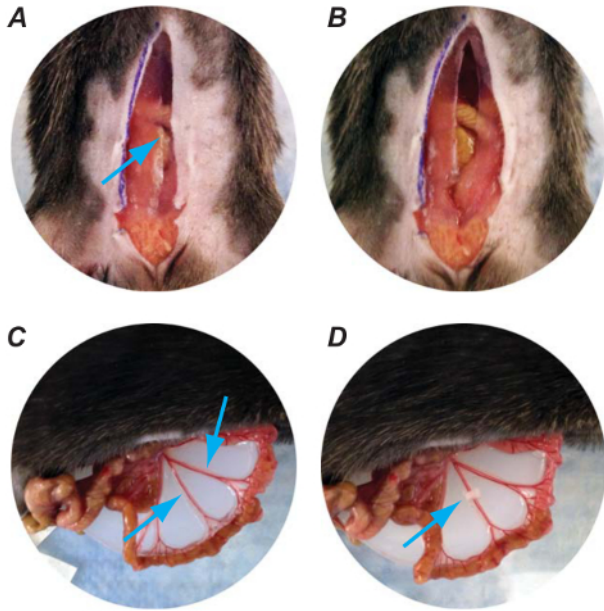
**Figure 4. Mesenteric Artery and Vein Thrombosis Model.** Exposure of mesenteric vessels as well as FeCl$_3$ treatment is shown. In **(A)**, the blue arrow indicates linea alba, the white fibrous tissue without vessel; In **(B)**, an incision cut alone the linea alba was shown; in **(C)**, the blue arrows indicate the second arch of the mesenteric arteries and veins; in **(D)**, the blue arrow indicates the filter paper situated with FeCl$_3$ solution. Please click here to view a larger version of this figure.
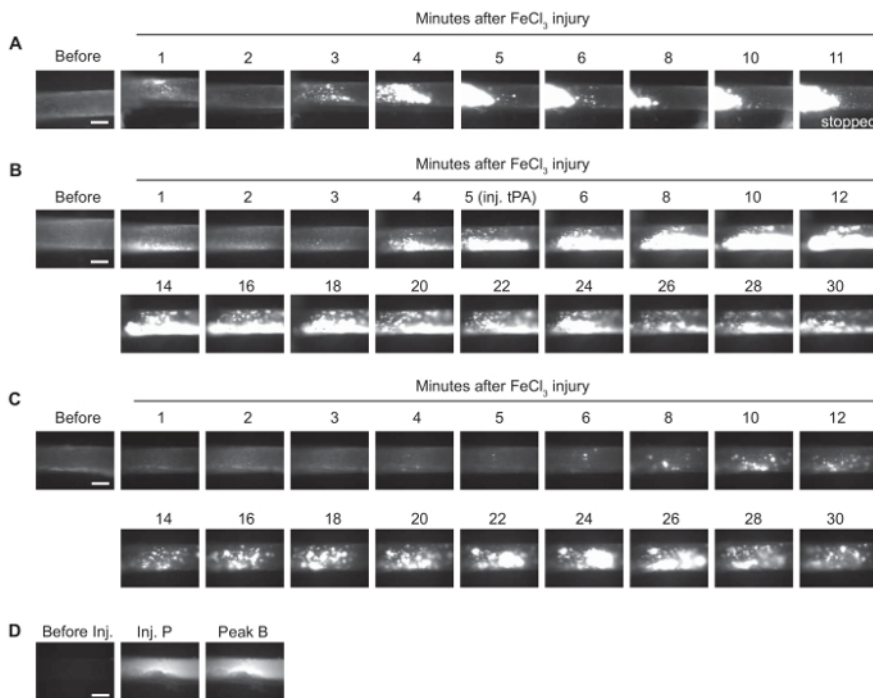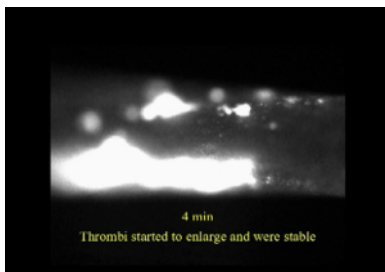

Figure 5. Representative Experiments using the Carotid Artery Thrombosis Model. **(A).** Thrombus formation in theC57Bl/6 mouse treated with 7.5% FeCl$_3$. **(B).** tPA mediated thrombolytic effect. **(C).** Injection of antibody targeting mouse thrombin receptor PAR4 on thrombosis was shown. **(D).** Thrombus-site-targeted nanovehicles specifically bind to actively forming thrombi was shown. Inj. P indicates injection of particle; and Peak B indicates peak banding of particles to the thrombi. All images were taken under same magnification. Scale bar = 300 μm. Please click here to view a larger version of this figure.
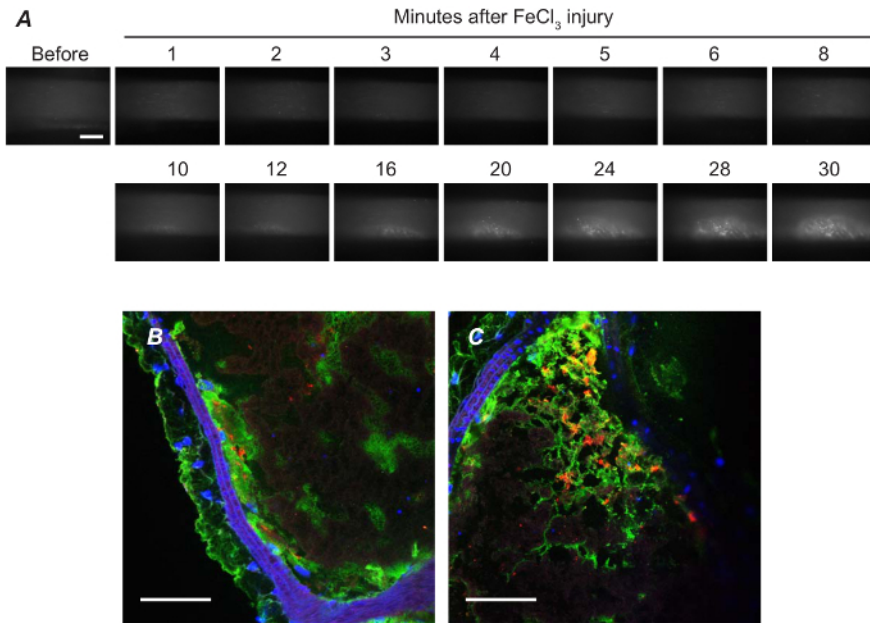
Figure 6. Role of RBC on Thrombus Formation. (A) Thrombocytopenic mice that received perfusion of DiI-labeled RBCs were subjected to the carotid artery thrombosis model and images after 7.5% FeCl$_3$ treatment were shown. Bar = 300 µm. **(B & C)** The injured carotid arteries were harvested, and frozen sections were prepared. Platelets were stained with CD41 (Green) and RBCs were shown as red (DiI). Nuclei were stained with DAPI. Vessels shown in **(B and C)** were from two different mice. Scale bars = 50 µm. Please click here to view a larger version of this figure.


Video 1: Representative video of the carotid artery thrombosis model in wild type (WT) mice. (Right-click to download.) This video shows the representative thrombus formation in the carotid artery of WT mice induced by topically applying filter paper situated with 7.5% FeCl$_3$ solution. Platelets were labelled by intravenous injection of rhodamine 6G, and video was taken in monochrome mode. The white mass is clotted platelets.
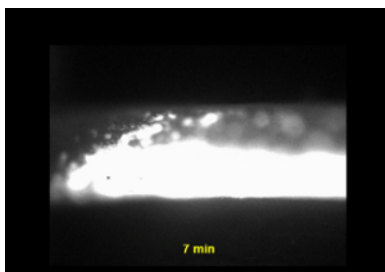

Video 2: Tissue plasminogen activator (tPA) mediated thrombolytic effect detected by the carotid artery thrombosis model. (Right-click to download.) Platelet labelling and thrombus formation were initiated as mentioned in video 1, and tPA was injected intravenously 5 min after 7.5% FeCl$_3$ injury.
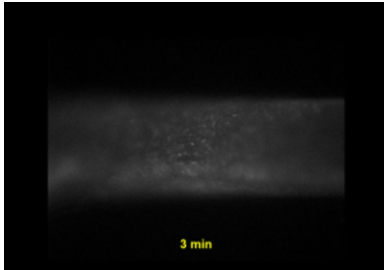
Video 3: Antiplatelet drug, namely anti-protease activated receptor 4 (PAR4) antibody, mediated anti-thrombotic effect detected by the carotid artery thrombosis model. (Right-click to download.) In this experiment, mice received PAR4 antibody and rhodamine 6G injection 10 min before thrombus formation was initiated by topically applying filter paper situated with 7.5% $FeCl_3$.
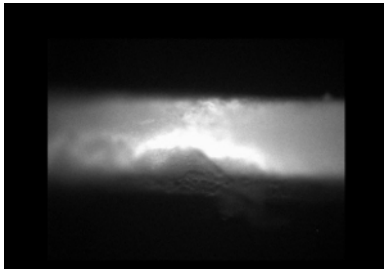
Video 4: Nanoparticle-mediated thrombi-specific targeting. (Right-click to download.) In this experiment, carotid artery thrombus formation was initiated with 7.5% $FeCl_3$ without labeling platelet. Nanoparticle was labeled with Rhodamine B and intravenously injected into the mouse 5 min after injury.
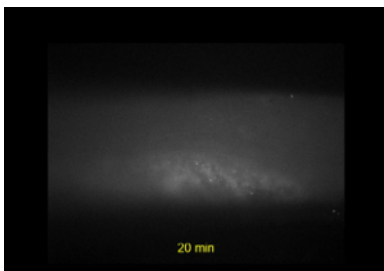
Video 5: Binding of the red blood cells detected by the carotid artery thrombosis model. (Right-click to download.) Red blood cells (RBCs) were labelled with 1,1'-Dioctadecyl-3,3,3',3'-Tetramethylindocarbocyanine Perchlorate (Dil, 10 µM final concentration), and 100 µl of the Dil-labeled RBCs (35% hematocrit) were injected into the thrombocytopenic mice. No platelet labeling was performed in this experiment. Thrombus was initiated as mentioned above with 7.5% $FeCl_3$.
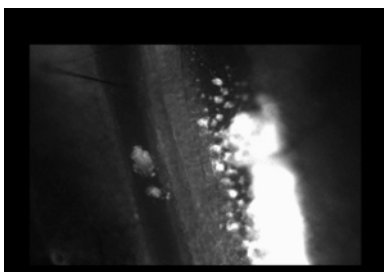
Video 6: Representative video of the mesenteric artery and vein thrombosis model on WT mice. (Right-click to download.) Platelets were labelled by intravenous injection of rhodamine 6G, and thrombus was initiated topically after applying one piece of filter paper with 12.5% $FeCl_3$ solution for 1 min. The vessel was observed under 10X dry lens.

Discussion

The $FeCl_3$-induced model is one of the most widely used thrombosis models, which can not only provide valuable information about genetic modifications on platelet function and thrombosis[7,8,16,19,31-33], but can also be a valuable tool for evaluation of therapeutic compounds and strategies for treatment and prevention of atherothrombotic diseases[11,17,34-37]. Here we have shown our modifications and refinements of this model and showed additional evidence of the utility of this technique, which is sufficiently sensitive to determine the effects of anticoagulant (tPA) and anti-platelet drugs (PAR4 antibody). In addition to the mechanistic study of thrombosis, the model can also be utilized to study nanotechnologies-based, thrombi-targeted drug delivery. It can also be used for detection of vessel wall reactive oxygen species (ROS) formation by injection of fluorescent ROS indicator[21].

Meticulous techniques are necessary to perform these models. The operator should have sufficient surgical skills as well as a deep understanding of vascular and blood cell biology. Several key points of the $FeCl_3$ induced carotid artery thrombosis model are[6]: (1) expose enough length of carotid artery (~5 mm) to allow application of the filter paper and leave a space to observe blood flow under intravital microscopy at late phase; (2) clearly strip the adventitial soft tissue around the carotid artery to allow the filter paper to contact the vessel wall directly and produce an even injury; (3) confirm no mechanical injury to the vessel wall and no thrombus formation before application of $FeCl_3$-saturated filter paper; (4) underlie the carotid artery with a piece of "U" shaped black plastic to separate the artery from surrounding tissue, to block background fluorescence, and to prevent $FeCl_3$ diffusion. By these strategies, we have generated highly reproducible data with the wild type C57Bl/6 mice, and in this mouse strain 7.5% $FeCl_3$ induced thrombosis time is 11.3 ± 3.16 min (n= 14)[6,7,19]. The jugular vein injection of rhodamine 6G to label circulating cells may be challenging. As an alternative, a tail vein injection can be performed before securing the mouse on the 15 cm plate lid. In comparing to the carotid artery model, the mesenteric artery and vein model is easier and less surgically intensive. However, as mentioned in the Result Section, due to the coverage of the vessels by fat tissue, the mesenteric thrombosis model is better for studying venous thrombosis but requires a larger sample size to minimize the error between different mice.

The limitation of this model is that the mechanism is not clear and still controversial. Initially, the mechanism of this model was believed to be that of $FeCl_3$ generated ROS induced denudation of endothelial cells, and subsequently led to exposure of blood components to the prothrombotic subendothelium, to render platelet adhesion, aggregation and thrombus formation[6,11]. By reconstitution of platelets pre-treated with GPVI antibody to the thrombocytopenic mice, we have demonstrated that the $FeCl_3$ model depends on platelet GPVI, and blocking platelet GPVI dramatically inhibited $FeCl_3$ induced thrombi formation[19]. This finding is in line with previous reports[38] and suggests that the $FeCl_3$ model may be more likely to mimic the pathophysiology of human atherosclerotic plaque rupture mediated thrombosis[6]. However, several recent studies have proposed new mechanisms including adhesion of red blood cells to the vessel wall as well as physiochemical effect of $FeCl_3$ induced aggregation of plasma proteins and blood cells[29,30]. These new insights suggest the potential mechanisms of this model may be more complex.

By perfusion of Dil-labeled RBCs into the thrombocytopenic mice and then inducing $FeCl_3$-triggered injury to the carotid artery with 7.5% $FeCl_3$, we found that the major cells adhering to the injured vessel walls are platelets (**Figure 6 and online video 5**). We did not find obvious RBCs adhesion, and the accumulation of RBCs in the thrombi seemed most likely to be a result of trapping. Our findings match the concepts of primary and secondary hemostasis[39]. The difference of our observation from the previous reports may be from hypoxia and hemodynamic change as in the study by Barr and colleagues[30], where the $FeCl_3$ injured carotid arteries for scanning electron microscopy examination were prepared in mice that had the left ventricle previously exposed without assistance of a mechanical ventillation. Blood oxygen concentration and hemodynamics will be dramatically decreased as both pulmonary and cardiac function will be affected immediately after the chest is opened without mechanical ventilation. Oxygen deprivation has long been associated with triggering of the procoagulant pathway and thrombosis[40] and also may enhance RBC adhesion. Another recent publication has shown that treatment of the carotid artery with a very high concentration of $FeCl_3$ (20%) for 5 or 10 min leads to a steady-state concentration of $FeCl_3$ at ~ 50 mM in the lumen of the injured vessel[29]. They thus directly infused 50 mM $FeCl_3$ into various blood components and examined the effect of $FeCl_3$ on aggregation ex vivo, which led them to propose a novel, 2-phase mechanism for the action of $FeCl_3$ in thrombus formation[29]. Although quite interesting, results from this study need to be interpreted with caution as it does not represent the $FeCl_3$ model commonly used. In contrast to the high concentration of $FeCl_3$ (20%, 1M as indicated in the paper) and long treatment (5 or 10 min), our previous studies as well as Barr et al. have demonstrated that 10% $FeCl_3$ treatment for 1 min is enough to induce rapid occlusive thrombus formation in the carotid artery within 7 min[6,30]. In addition, in most of the experiments using the $FeCl_3$ model, a further low concentration of $FeCl_3$ (5 - 7.5%) is used.

Another limitation of this model is that due to the severe oxidative injury to the endothelium as well as endothelial denudation post-$FeCl_3$ treatment, this model may be not a proper tool to study endothelial inflammation associated thrombosis. However, by using these techniques to prepare the carotid artery in combination with perfusion of fluorescently labeled leukocytes, we can test the adhesion and rolling of the leukocytes on the inflammatory endothelium[41].

In summary, we have refined and standardized the $FeCl_3$-induced vascular injury model to produce a highly reproducible injury on the carotid artery and quantitate blood flow cessation time accurately by intravital microscopy. This model is sufficient and sensitive to test the anticoagulant and antiplatelet drugs, and is also suitable for studies of thrombi-targeted nanomedicine. In combination with bone marrow transplantation, platelet infusion into the thrombocytopenic mice or direct intravascular injection of candidate drugs, we have demonstrated that this is a convenient, simple and sensitive tool to study thrombosis in vivo[7-10,16,19,42,43].

Disclosures

The authors have nothing to disclose.

Acknowledgements

References

1. Sachs, U. J., & Nieswandt, B. *In vivo* thrombus formation in murine models. *Circ Res.* **100**, 979-991 (2007).
2. Libby, P., Lichtman, A. H., & Hansson, G. K. Immune effector mechanisms implicated in atherosclerosis: from mice to humans. *Immunity.* **38**, 1092-1104 (2013).
3. Ruggeri, Z. M. Platelet adhesion under flow. *Microcirculation.* **16**, 58-83 (2009).
4. Watson, S. P. Platelet activation by extracellular matrix proteins in haemostasis and thrombosis. *Curr Pharm Des.* **15**, 1358-1372 (2009).
5. Furie, B., & Furie, B. C. Thrombus formation *in vivo*. *J Clin Invest.* **115**, 3355-3362 (2005).

6. Li, W., McIntyre, T. M., & Silverstein, R. L. Ferric chloride-induced murine carotid arterial injury: A model of redox pathology. *Redox Biol.* **1**, 50-55 (2013).
7. Ghosh, A. *et al.* Platelet CD36 mediates interactions with endothelial cell-derived microparticles and contributes to thrombosis in mice. *J Clin Invest.* **118**, 1934-1943 (2008).
8. Chen, K. *et al.* Vav guanine nucleotide exchange factors link hyperlipidemia and a prothrombotic state. *Blood.* (2011).
9. Li, W. *et al.* CD36 participates in a signaling pathway that regulates ROS formation in murine VSMCs. *J Clin Invest.* **120**, 3996-4006 (2010).
10. Chen, K., Febbraio, M., Li, W., & Silverstein, R. L. A specific CD36-dependent signaling pathway is required for platelet activation by oxidized low-density lipoprotein. *Circ Res.* **102**, 1512-1519 (2008).
11. Kurz, K. D., Main, B. W., & Sandusky, G. E. Rat model of arterial thrombosis induced by ferric chloride. *Thromb Res.* **60**, 269-280 (1990).
12. Konstantinides, S., Schafer, K., Thinnes, T., & Loskutoff, D. J. Plasminogen activator inhibitor-1 and its cofactor vitronectin stabilize arterial thrombi after vascular injury in mice. *Circulation.* **103**, 576-583 (2001).
13. Leadley, R. J., Jr. *et al.* Pharmacodynamic activity and antithrombotic efficacy of RPR120844, a novel inhibitor of coagulation factor Xa. *J Cardiovasc Pharmacol.* **34**, 791-799 (1999).
14. Marsh Lyle, E. *et al.* Assessment of thrombin inhibitor efficacy in a novel rabbit model of simultaneous arterial and venous thrombosis. *Thromb Haemost.* **79**, 656-662 (1998).
15. Farrehi, P. M., Ozaki, C. K., Carmeliet, P., & Fay, W. P. Regulation of arterial thrombolysis by plasminogen activator inhibitor-1 in mice. *Circulation.* **97**, 1002-1008 (1998).
16. Robertson, J. O., Li, W., Silverstein, R. L., Topol, E. J., & Smith, J. D. Deficiency of LRP8 in mice is associated with altered platelet function and prolonged time for *in vivo* thrombosis. *Thromb Res.* **123**, 644-652 (2009).
17. Gupta, N., Li, W., Willard, B., Silverstein, R. L., & McIntyre, T. M. Proteasome proteolysis supports stimulated platelet function and thrombosis. *Arterioscler Thromb Vasc Biol.* **34**, 160-168 (2014).
18. Srikanthan, S., Li, W., Silverstein, R. L., & McIntyre, T. M. Exosome poly-ubiquitin inhibits platelet activation, downregulates CD36 and inhibits pro-atherothombotic cellular functions. *J Thromb Haemost.* **12**, 1906-1917 (2014).
19. Li, W. *et al.* Thymidine phosphorylase participates in platelet signaling and promotes thrombosis. *Circ Res.* **115**, 997-1006 (2014).
20. Le Menn, R., Bara, L., & Samama, M. Ultrastructure of a model of thrombogenesis induced by mechanical injury. *J Submicrosc Cytol.* **13**, 537-549 (1981).
21. Li, W. *et al.* CD36 participates in a signaling pathway that regulates ROS formation in murine VSMCs. *J Clin Invest.* **120**, 3996-4006 (2010).
22. Re-examining Acute Eligibility for Thrombolysis Task Force. *et al.* Review, historical context, and clarifications of the NINDS rt-PA stroke trials exclusion criteria: Part 1: rapidly improving stroke symptoms. *Stroke.* **44**, 2500-2505 (2013).
23. Mumaw, M. M., de la Fuente, M., Arachiche, A., Wahl, J. K., 3rd & Nieman, M. T. Development and characterization of monoclonal antibodies against Protease Activated Receptor 4 (PAR4). *Thromb Res.* **135**, 1165-1171 (2015).
24. Mumaw, M. M., de la Fuente, M., Noble, D. N., & Nieman, M. T. Targeting the anionic region of human protease-activated receptor 4 inhibits platelet aggregation and thrombosis without interfering with hemostasis. *J Thromb Haemost.* **12**, 1331-1341 (2014).
25. Modery-Pawlowski, C. L., Kuo, H. H., Baldwin, W. M., & Sen Gupta, A. A platelet-inspired paradigm for nanomedicine targeted to multiple diseases. *Nanomedicine (Lond).* **8**, 1709-1727 (2013).
26. Anselmo, A. C. *et al.* Platelet-like nanoparticles: mimicking shape, flexibility, and surface biology of platelets to target vascular injuries. *ACS Nano.* **8**, 11243-11253 (2014).
27. Modery, C. L. *et al.* Heteromultivalent liposomal nanoconstructs for enhanced targeting and shear-stable binding to active platelets for site-selective vascular drug delivery. *Biomaterials.* **32**, 9504-9514 (2011).
28. Woollard, K. J., Sturgeon, S., Chin-Dusting, J. P., Salem, H. H., & Jackson, S. P. Erythrocyte hemolysis and hemoglobin oxidation promote ferric chloride-induced vascular injury. *J Biol Chem.* **284**, 13110-13118 (2009).
29. Ciciliano, J. C. *et al.* Resolving the multifaceted mechanisms of the ferric chloride thrombosis model using an interdisciplinary microfluidic approach. *Blood.* **126**, 817-824 (2015).
30. Barr, J. D., Chauhan, A. K., Schaeffer, G. V., Hansen, J. K., & Motto, D. G. Red blood cells mediate the onset of thrombosis in the ferric chloride murine model. *Blood.* **121**, 3733-3741 (2013).
31. Dunne, E. *et al.* Cadherin 6 has a functional role in platelet aggregation and thrombus formation. *Arterioscler Thromb Vasc Biol.* **32**, 1724-1731 (2012).
32. Lockyer, S. *et al.* GPVI-deficient mice lack collagen responses and are protected against experimentally induced pulmonary thromboembolism. *Thromb Res.* **118**, 371-380 (2006).
33. Zhou, J. *et al.* The C-terminal CGHC motif of protein disulfide isomerase supports thrombosis. *J Clin Invest.* **2015** (2015).
34. Eckly, A. *et al.* Mechanisms underlying FeCl3-induced arterial thrombosis. *J Thromb Haemost.* **9**, 779-789 (2011).
35. Day, S. M., Reeve, J. L., Myers, D. D., & Fay, W. P. Murine thrombosis models. *Thromb Haemost.* **92**, 486-494 (2004).
36. Cooley, B. C. Murine models of thrombosis. *Thromb Res.* **129 Suppl 2**, S62-64 (2012).
37. Gupta, N., Li, W., & McIntyre, T. M. Deubiquitinases Modulate Platelet Proteome Ubiquitination, Aggregation, and Thrombosis. *Arterioscler Thromb Vasc Biol.* **35**, 2657-2666 (2015).
38. Konstantinides, S. *et al.* Distinct antithrombotic consequences of platelet glycoprotein Ibalpha and VI deficiency in a mouse model of arterial thrombosis. *J Thromb Haemost.* **4**, 2014-2021 (2006).
39. Versteeg, H. H., Heemskerk, J. W., Levi, M., & Reitsma, P. H. New fundamentals in hemostasis. *Physiol Rev.* **93**, 327-358 (2013).
40. Yan, S. F., Mackman, N., Kisiel, W., Stern, D. M., & Pinsky, D. J. Hypoxia/Hypoxemia-Induced activation of the procoagulant pathways and the pathogenesis of ischemia-associated thrombosis. *Arterioscler Thromb Vasc Biol.* **19**, 2029-2035 (1999).
41. Rahaman, S. O., Li, W., & Silverstein, R. L. Vav Guanine nucleotide exchange factors regulate atherosclerotic lesion development in mice. *Arterioscler Thromb Vasc Biol.* **33**, 2053-2057 (2013).
42. Silverstein, R. L., Li, W., Park, Y. M., & Rahaman, S. O. Mechanisms of cell signaling by the scavenger receptor CD36: implications in atherosclerosis and thrombosis. *Trans Am Clin Climatol Assoc.* **121**, 206-220 (2010).
43. Liu, J., Li, W., Chen, R., & McIntyre, T. M. Circulating biologically active oxidized phospholipids show on-going and increased oxidative stress in older male mice. *Redox Biol.* **1**, 110-114 (2013).